Zoomorphology (1998) 118:207–223

ORIGINAL ARTICLE

Myriam Verstappen · Peter Aerts · Frits De Vree

Functional morphology of the hindlimb musculature of the black-billed magpie, *Pica pica* (Aves, Corvidae)

Accepted: 26 June 1998

Abstract In spite of the ecological relevance of terrestrial locomotion for many bird species, this function remains poorly studied to date. Gait preferences and transitions seem present, but it is not known which factors might determine the running style. Morphological and morphometric data needed for further biomechanical modelling are presented for the black-billed magpie (*Pica pica*), a species which walks, runs and hops. Detailed descriptions of the muscle–tendon systems and the attachment sites on the hindlimb skeleton are given. Pinnation angles, fibre lengths and muscle masses are determined. From the latter two, physiological cross-sections of the muscle bundles are calculated. Tendon ossifications are qualitatively scored. Further, information on the mechanical variables of the body segments are collected (i.e. mass, length, position of the centre of gravity and moment of inertia of digits, tarsometatarsus, lower leg, upper leg, body, and head/neck). Moment arms of the important muscles powering terrestrial locomotion are discussed and, for some upper leg muscles, an equation to calculate the moment arms as a function of knee and hip joint angles is presented. All these data are indispensable for further kinesiological research.

A. Introduction

Most of the studies dealing with terrestrial locomotion concentrate on mammals, including humans (e.g. Cavagna et al. 1977; Winter 1990a, b; Alexander 1992; Bennett 1992). The kinematics and dynamics of terrestrial locomotion of birds have been studied in a quantitative way in only a few cases (Cracraft 1971; Rylander and Bolen 1974; Clark and Alexander 1975; Cavagna et al. 1977; Dagg 1977; Alexander et al. 1979; Hayes and Alexander 1983; Roberts et al. 1997). Although most research on birds focused on flying, it can be argued that terrestrial locomotion is an important ecological function for many birds and, thus, also merits study. Some bird species have lost the ability to fly (e.g. Struthioniformes) or rarely use it (e.g. Galliformes), while many others spend a great deal of their time on the ground, mainly to feed [e.g. scavenging, like corvids, and birds eating soil organisms such as starlings (*Sturnus vulgaris*[1])].

Like mammals, birds use different gaits: they walk, run and hop. However, a distinct relation between (relative) velocity and gait transition as found in mammals (e.g. Hoyt and Taylor 1981; Farley and Taylor 1991; Alexander 1992; Hreljac 1993a, b, 1995a, b; Kram et al. 1997) and in some Archosauria and Lepidosauria (e.g. crocodiles: Webb and Gans 1982; Lacertids: own observations) seems far from obvious. Some species only hop (e.g. *Passer domesticus*: Kunkel 1962; Clark 1975; own observations) whereas others walk and run (e.g. *Sturnus vulgaris*: Kunkel 1962; own observations) or walk and hop (e.g. *Corvus monedula*: Kunkel 1962; own observations), and still others use all three gaits (e.g. *Pica pica*: Hayes and Alexander 1983; own observations).

Our study seeks to understand which mechanical factors determine the choice of, and transition among gaits in birds. As a first step, the magpie (*Pica pica*) is chosen as a model. These birds walk, run and hop, and are fairly manageable for kinesiological experiments. Primary interest goes to the propulsion dynamics of straight forward locomotion at constant speeds, as this will allow direct comparison and integration with former, important experimental and theoretical work on terrestrial locomotion (Alexander 1974, 1976, 1977a, b, 1992; Alexander and Vernon 1975; Clark and Alexander 1975; Alexander et al. 1980; Mochon and McMahon 1980; McMahon 1984; Blickhan 1989; Mi-netti and Saibene 1992; Farley et al. 1993; Minetti and Alexander 1997). However, biomechanical analysis of the terrestrial locomotion requires profound knowledge of the morphology and mor-

M. Verstappen (✉) · P. Aerts · F. De Vree
Department of Biology, University of Antwerp (UIA),
Universiteitsplein 1, B-2610 Antwerpen, Belgium
e-mail: vstappen@uia.ua.ac.be,
Tel.: 32(0)38202260, Fax: 32(0)38202271

[1] Nomenclatural authors and dates of publication of scientific names are not given in this paper; instead, we refer to Peters (1987), Checklist of birds of the world

phometry of the hindlimb. Thus, this paper deals with the musculoskeletal system of the magpie's leg.

B. Materials and methods

Dead specimens of black-billed magpie (*Pica pica*) were provided by official game keepers in Flanders (Belgium). Dissection of the hindlimbs (specimens 1–4, see Table 1) was performed with the aid of a stereomicroscope (WILD M3Z), and a camera lucida was used to make the illustrations. Muscles or muscle bundles were grouped per limb segment and described from superficial to deeper layers, starting from a lateral view. Within each layer, muscles are described in alphabetical order. Muscles which can only be seen from the medial side were described under a separate heading. The nomenclature follows that of the *Nomina Anatomica Avium* (Baumel et al. 1993). All abbreviations used are explained in Table 6. A skeletal preparation of the leg and pelvic girdle of specimen 4 (Table 1) was made and used to mark the origin and insertion of the muscles and tendons. Positions of the attachment sites were represented on a scale drawing (see Figs. 5, 6).

The physiological cross-sections (= muscle volume/mean fibre length) of the muscles or muscle bundles of specimen 3 (Table 1) were calculated. Muscle volume was obtained from mass and density of muscle tissue (1050 kg/m^3; Alexander 1983; Taylor 1994). To determine the mean muscle fibre length, the separate muscles (or bundles) were kept in a 30% HNO_3 solution for 24 h to dissolve the connective tissue (Loeb and Gans 1986). Forty fibres were then collected at random, measured (computer digitisation) and averaged.

On a longitudinal section through the muscle belly, pinnation angles for 10–15 fibres chosen at equal intervals along the internal tendon sheet were measured and averaged (Table 6). Lengths of external and internal tendon sheets (if present) were also determined (Table 6). Tendon ossification was qualitatively scored by manipulation. The length of the ossified part of the external tendon is mentioned (as a percentage of the total external tendon length) in Table 6.

In Table 6, a code is added to indicate the position of each muscle with respect to the crossed joint. Intraphalangeal joints were not considered. This code is compiled as follows. The first capital represents the joint (H: hip, K: knee, A: ankle, I: interdigital joint). Subscripts indicate positions (Cr: cranial, Ca: caudal, P: proximal, D: distal, M: medial, L: lateral; positional references are according to Baumel et al. 1993). As an example, the code K_{LCa}/A_{Ca} of a biarticular calf muscle reads as follows: the knee is crossed laterocaudally, and the ankle is crossed caudally.

Moment arms of muscles vary according the particular configuration of the leg segments at any instant of the locomotion cycle. In the Discussion, a formula is presented to estimate the length of the moment arm based on the knee and hip angle. Parameter values for six muscles (see Table 7) were recalculated from the digitisation (Houston Instruments HIPAD) of the centres of the attachment sites of the involved muscles as presented on Fig. 6 (see Discussion).

The body segments of three other adult specimens (specimens 5–7, see Table 1) (head – neck, trunk – wings, tail, upper leg, lower leg, tarsometatarsus and digits) were divided at the joints, and their length and mass were determined (Tables 2, 3). Position of the centre of mass (COM; as a percentage of segment length, Table 4) and moment of inertia (MOI, Table 5) of all segments except the digits were determined for specimen 7. A suspension method was used to estimate the COM (Alexander 1983); the MOI was measured by means of a pendulum (Alexander 1983; Smith 1987). The moment of inertia reflects the tendency of a body to resist accelerated rotations about a specific axis. This is equivalent to mass in rectilinear motion.

Table 1 Mass, body and tarsometatarsus length for dissected birds (specimens 1–4) and those used for division into body segments (specimens 5–7)

Specimen	Mass (g)	Body length (cm)	Tarsometatarsus length (cm)
1	203	17.6	4.7
2	162	14.4	4.6
3	185	19.4	4.6
4	181	19.5	4.6
5	219	17.8	5.0
6	167	15.8	4.8
7	199	19.1	4.7

C. Results

I. Morphology

1. Muscles associated with the thigh (femur, Fig. 1)

a) Superficial layer. M. flexor cruris lateralis: Most of the fibres of the M. flexor cruris lateralis pars pelvica (*MFCLP*, Figs. 3B, 6A, D) originate muscular from the caudal part of the lateral crest of the ilium, just caudal to the ilioischiadic foramen. The caudalmost fibres of this muscle arise by an aponeurosis that passes over the lateral surface of the ilium to the transverse process of the cranial caudal vertebra. The parallel-fibred bundle runs

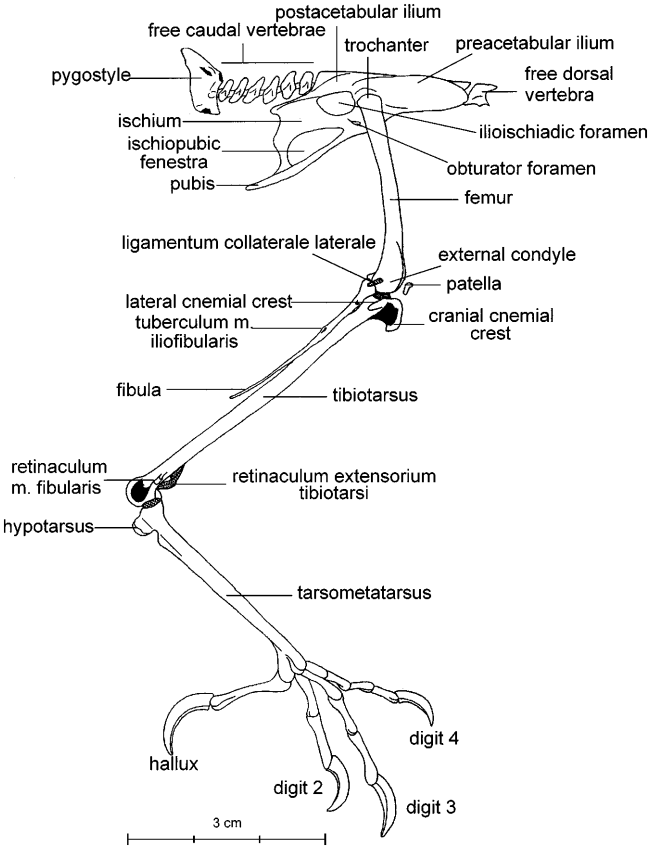

Fig. 1 *Pica pica*, lateral view of the hindlimb skeleton

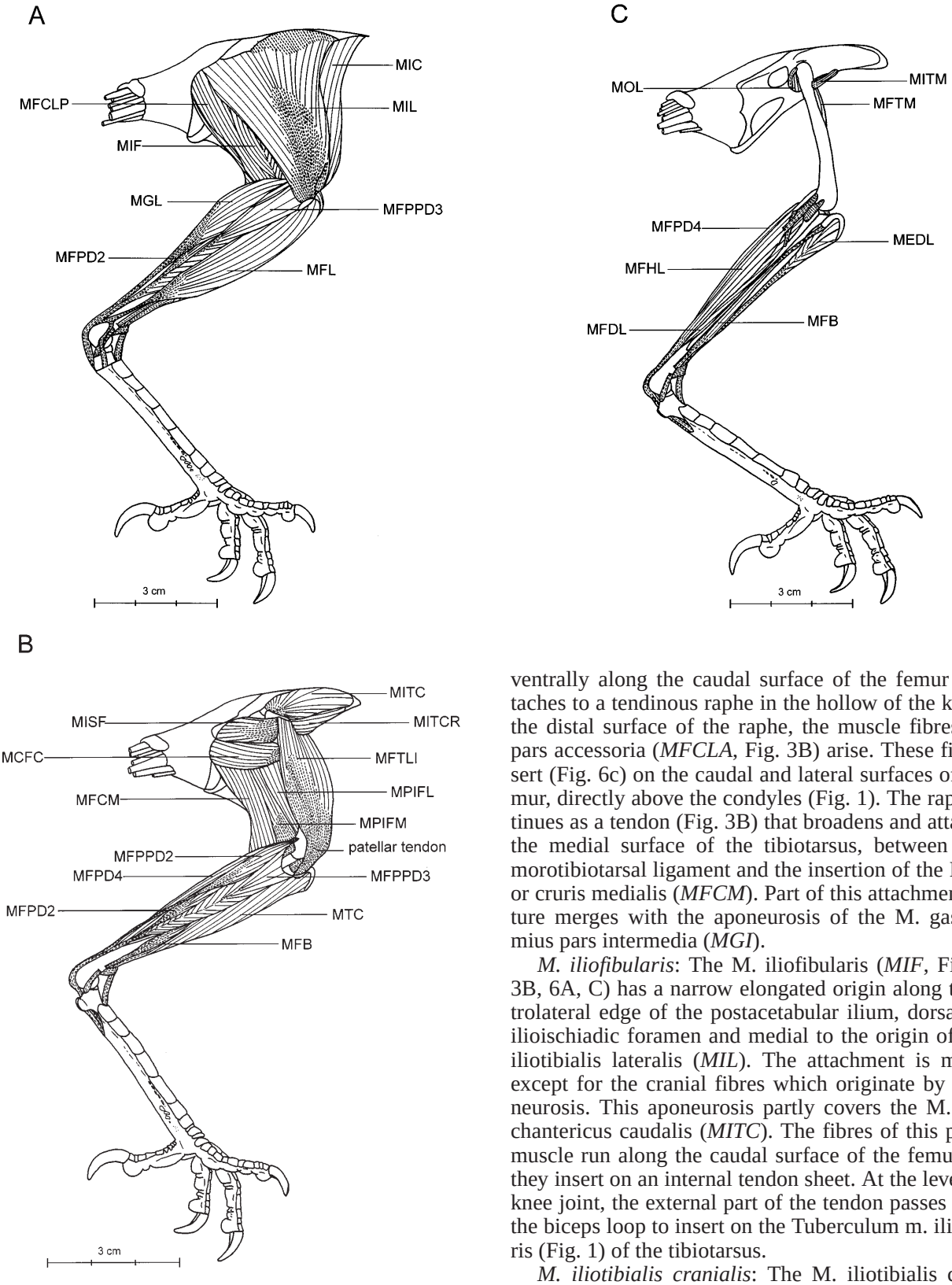

Fig. 2A–C *Pica pica*, hindlimb musculature: lateral view. **A** after removal of the skin. **B** after removal of the MFCL, MFL, MGL, MGM, MIC, MIF and MIL. **C** After removal of the MCFC, MFCM, MFPD2, MFPPD2, MFPPD3, MFTLI, MISF, MITC, MITCR, MPIFM, MPIFL and MTC. For explanation of abbreviations, see Table 6

ventrally along the caudal surface of the femur and attaches to a tendinous raphe in the hollow of the knee. On the distal surface of the raphe, the muscle fibres of the pars accessoria (*MFCLA*, Fig. 3B) arise. These fibres insert (Fig. 6c) on the caudal and lateral surfaces of the femur, directly above the condyles (Fig. 1). The raphe continues as a tendon (Fig. 3B) that broadens and attaches to the medial surface of the tibiotarsus, between the femorotibiotarsal ligament and the insertion of the M. flexor cruris medialis (*MFCM*). Part of this attachment structure merges with the aponeurosis of the M. gastrocnemius pars intermedia (*MGI*).

M. iliofibularis: The M. iliofibularis (*MIF*, Figs. 2A, 3B, 6A, C) has a narrow elongated origin along the ventrolateral edge of the postacetabular ilium, dorsal to the ilioischiadic foramen and medial to the origin of the M. iliotibialis lateralis (*MIL*). The attachment is muscular except for the cranial fibres which originate by an aponeurosis. This aponeurosis partly covers the M. iliotrochantericus caudalis (*MITC*). The fibres of this pinnated muscle run along the caudal surface of the femur where they insert on an internal tendon sheet. At the level of the knee joint, the external part of the tendon passes through the biceps loop to insert on the Tuberculum m. iliofibularis (Fig. 1) of the tibiotarsus.

M. iliotibialis cranialis: The M. iliotibialis cranialis (*MIC*, Figs. 2A, 3A, 6A) constitutes the cranial aspect of the thigh. The parallel-fibred muscle arises muscularly from the craniodorsal edge of the preacetabular ilium, except for a few fibres that arise aponeurotically from the spinous process of the last free dorsal vertebra (Fig. 1).

The muscle fibres run to the tibiotarsus, just below the knee joint, where they insert partly muscularly and partly aponeurotically via the patellar tendon (insertion site: Fig. 6C). The caudal fibres of the cranial part are tightly connected with the cranial fibres of the M. iliotibialis lateralis (*MIL*). Some fibres are attached to the surface aponeurosis of the M. femorotibialis medialis.

M. iliotibialis lateralis: M. iliotibialis lateralis (*MIL*, Figs. 2A, 3B, 6A) originates from a narrow elongated area along almost the entire length of the ilium, between the origins of the M. iliotibialis cranialis (*MIC*) and M. flexor cruris lateralis pars pelvica (*MFCLP*). Cranially, muscle fibres attach to the dorsal side of the ilium by an aponeurosis that covers the M. iliotrochantericus caudalis (*MITC*) almost completely. The muscle fibres converge towards an aponeurosis that is common with the M. femorotibialis lateralis et intermedius (*MFTLI*). This aponeurosis merges into the patellar tendon (insertion site: Fig. 6C) which inserts on the dorsal edge of the lateral cnemial crest of the tibiotarsus.

b) Medial layer. M. caudofemoralis pars caudalis: The M. caudofemoralis pars caudalis (*MCFC*, Figs. 2B, 3A, B, 6C) originates by a narrow tendon from the lateroventral surface of the pygostyle. The muscle belly runs cranially along the ventral surface of the M. ischiofemoralis (*MISF*) and passes between Mm. flexor cruris lateralis pars pelvica (*MFCLP*) and flexor cruris medialis (*MFCM*) to insert tendinously on the caudolateral surface of the femur just below the trochanter. At its insertion, the muscle is covered by the M. iliofibularis (*MIF*).

M. femorotibialis lateralis et intermedius: M. femorotibialis lateralis et intermedius (*MFTLI*, Figs. 2B, 3A, B) originates partly muscularly and partly aponeurotically from almost the entire craniolateral and craniomedial surface of the femur. The two parts (*MFTL*, Fig. 6A; *MFTM*, Fig. 6B) are tightly connected by an internal aponeurotic sheath that is attached to the cranial surface of the femur shank, but their heads are separated by the Mm. iliotrochantericus cranialis (*MITCR*) and medius (*MITM*). The muscle fibres run ventrally to insert on a large aponeurosis that merges into the patellar tendon which also serves as the insertion site (Fig. 6C) of the M. iliotibialis lateralis.

M. flexor cruris medialis: The M. flexor cruris medialis (*MFCM*, Figs. 2B, 3A, 6A, D) is the caudalmost muscle of the thigh. It arises muscularly from the caudolateral surface of the ischium. A few fibres attach to the aponeurosis of the abdominal muscles (M. pubocaudalis externus) just behind the ischium. The parallel-fibred M. flexor cruris medialis inserts by a wide tendon sheet on the proximal part of the medial surface of the tibiotarsus. This sheet passes between the pars intermedia (*MGI*) and pars medialis (*MGM*) of the M. gastrocnemius. Just before the insertion, the flexor cruris lateralis and medialis partly fuse.

M. iliotrochantericus caudalis: The M. iliotrochantericus caudalis (*MITC*, Figs. 2B, 6A, C) is the largest muscle of the iliotrochantericus group and originates muscularly from almost the entire lateral surface of the preacetabular ilium. The fibres of the fan-shaped muscle run caudolaterally to attach to the dorsolateral edge of the trochanter by a short tendon.

M. iliotrochantericus cranialis: The M. iliotrochantericus cranialis (*MITCR*, Figs. 2B, 3A, B, 6A, C) arises mainly muscularly from a narrow strip on the cranioventral edge of the preacetabular ilium, just in front of the origin of the M. iliotrochantericus medius (*MITM*). The muscle inserts by a short tendon on the craniolateral surface of the trochanter. As mentioned, this insertion tendon passes between the two heads of the M. femorotibialis lateralis et intermedius (*MFTLI*) and lies ventral to that of the M. iliotrochantericus medius.

M. ischiofemoralis: The M. ischiofemoralis (*MISF*, Figs. 2B, 3A, B, 6A, C) lies dorsally to the M. caudofemoralis pars caudalis (*MCFC*) and arises muscularly from the lateral surface of the ischium, between the ilioischiadic foramen, the lateral crest of the ilium and the ischiopubic fenestra. The muscle fibres converge to a small aponeurotic plate that attaches to the caudolateral surface of the femur, just below the trochanter.

M. puboischiofemoralis pars lateralis: The parallel fibred M. puboischiofemoralis pars lateralis (*MPIFL*, Figs. 2B, 3A, 6A, D) is a flat and broad muscle that arises mainly muscularly from a narrow area on the craniolateral surface of the ischium, between the caudoventral edge of the obturator foramen and the cranial half of the dorsal edge of the ischiopubic fenestra. The long muscle fibres run to the caudal surface of the distal two-thirds of the femur, up to the caudomedial border of the internal condyle.

M. puboischiofemoralis pars medialis: The M. puboischiofemoralis pars medialis (*MPIFM*, Figs. 2B, 3A, 6A, D) is a flat, broad muscle that originates from a narrow area on the caudolateral surface of the ischium, extending along the caudal half of the dorsal edge of the ischiopubic fenestra, just caudal to the origin of the M. puboischiofemoralis pars lateralis (*MPIFL*). Cranially, the fibres originate muscularly whereas the caudal half of the muscle originates from an aponeurosis. A few deeper fibres originate from the membrane that covers the ischiopubic fenestra. The muscle inserts muscularly and aponeurotically on the caudomedial surface of the internal condyle of the femur.

c) Deep layer. M. femorotibialis medialis: The M. femorotibialis medialis (*MFTM*, Figs. 3A, 6B, D) arises muscularly from almost the entire medial surface of the femur. Halfway along the femur, the muscle divides into two parts. The fibres of the two parts run ventrally to merge into a tendon and attach to the craniomedial surface of the head of the tibiotarsus. The longer tendon of the deepest part inserts more proximally than the smaller tendon of the superficial part. The insertions are covered by the proximal part of the M. gastrocnemius pars medialis (*MGM*).

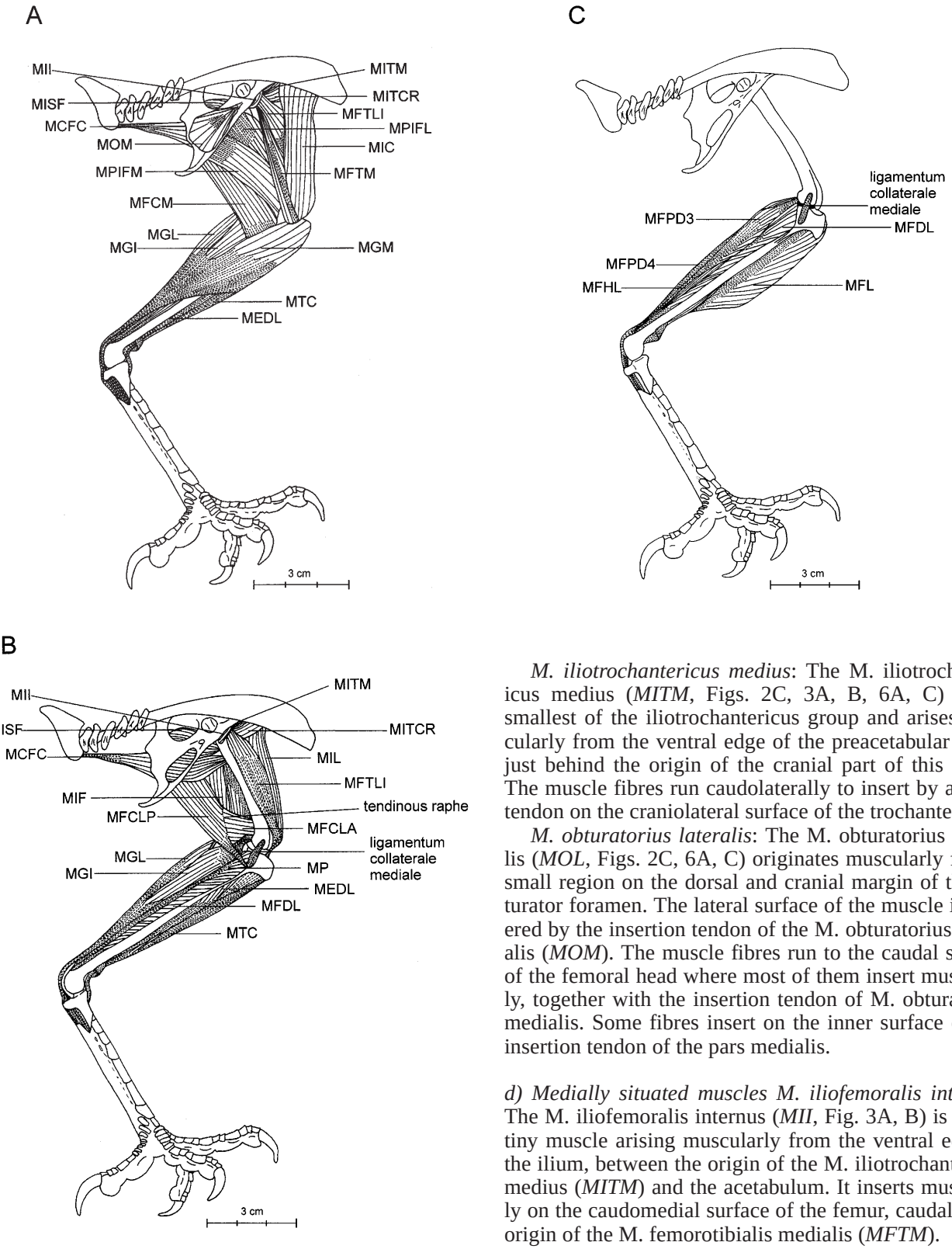

Fig. 3A–C *Pica pica*, hindlimb musculature: medial view. **A** After removal of the skin. **B** After removal of the MFCM, MFTM, MGM, MIC, MOM, MPIFM, MPIFL. **C** After removal of the MCFC, MEDL, MFCL, MFTLI, MGI, MGL, MIF, MII, MIL, MISF, MITC, MITCR, MITM, MP, MTC. For explanation of abbreviations, see Table 6

M. iliotrochantericus medius: The M. iliotrochantericus medius (*MITM*, Figs. 2C, 3A, B, 6A, C) is the smallest of the iliotrochantericus group and arises muscularly from the ventral edge of the preacetabular ilium, just behind the origin of the cranial part of this group. The muscle fibres run caudolaterally to insert by a small tendon on the craniolateral surface of the trochanter.

M. obturatorius lateralis: The M. obturatorius lateralis (*MOL*, Figs. 2C, 6A, C) originates muscularly from a small region on the dorsal and cranial margin of the obturator foramen. The lateral surface of the muscle is covered by the insertion tendon of the M. obturatorius medialis (*MOM*). The muscle fibres run to the caudal surface of the femoral head where most of them insert muscularly, together with the insertion tendon of M. obturatorius medialis. Some fibres insert on the inner surface of this insertion tendon of the pars medialis.

d) Medially situated muscles M. iliofemoralis internus: The M. iliofemoralis internus (*MII*, Fig. 3A, B) is a very tiny muscle arising muscularly from the ventral edge of the ilium, between the origin of the M. iliotrochantericus medius (*MITM*) and the acetabulum. It inserts muscularly on the caudomedial surface of the femur, caudal to the origin of the M. femorotibialis medialis (*MFTM*).

M. obturatorius medialis: The M. obturatorius medialis (*MOM*, Figs. 3A, 6B, C) is a flat, pinnated, triangular muscle situated on the medial surface of the pelvic girdle. The muscle fibres originate from an area around the ischiopubic fenestra, that is entirely covered by the mus-

cle. They converge towards an internal aponeurosis that merges in an external tendon when passing through the obturator foramen. The tendon inserts on the caudolateral surface of the trochanter, together with the M. obturatorius lateralis.

2. Muscles associated with the lower leg (tibiotarsus and fibula, Fig. 1)

a) Superficial layer. M. fibularis longus: The M. fibularis longus (*MFL*, Figs. 2A, 3C, 6A) originates muscularly from a narrow line between and on the inner surface of the lateral and cranial cnemial crests of the tibiotarsus, just above the origin of the M. tibialis cranialis pars tibialis (*MTCT*) and below the insertion of the patellar tendon. Some fibres originate from the joint ligaments of the knee. The muscle runs along the lateral surface of the lower leg towards the ankle joint, and the fibres of the deep layer are tightly connected to the M. tibialis cranialis. Just above the ankle joint, the tendon of the M. fibularis longus bifurcates, with the shorter, caudal branch extending to the proximolateral edge of the Cartilago tibialis. The longer, cranial branch passes downwards, laterally to the ankle joint, to the caudolateral surface of the tarsometatarsus. Just below the hypotarsus, the tendon attaches to the lateral edge of the tendon of the M. flexor perforatus digiti 3 (*MFPD3*).

M. flexor perforans et perforatus digiti 3: The M. flexor perforans et perforatus digiti 3 (*MFPPD3*, Figs. 2A, B, 4, 5D, 6A) covers the lateral surface of the tibiotarsus. The muscle originates: (1) from the upper part of the fibular ligament and from the external femoral condyle by a tendon that also serves as the origin of the Mm. flexor hallucis longus (*MFHL*), flexor perforans et perforatus digiti 2 (*MFPPD2*) and flexor perforatus digiti 2 (*MFPD2*), (2) from the medial surface of the lateral cnemial crest and (3) from the proximal end of the fibula next to the attachment of the fibular ligament. The pinnated muscle merges into a tendon that first passes through the Cartilago tibialis, beneath the Achilles tendon and lateral to the tendon of the M. flexor perforans et perforatus digiti 2, and then through an ossified channel in the hypotarsus, caudal to that of the M. flexor perforans et perforatus digiti 2 and medial to the channel from the M. flexor perforatus digiti 4 (*MFPD4*, Fig. 4). The tendon continues along the caudal surface of the tarsometatarsus toward the plantar surface of the third digit where it perforates the tendon of the M. flexor perforatus digiti 3 (*MFPD3*) at the base of the first phalanx. The tendon of the M. perforans et perforatus digiti 3 itself is perforated by a branch of the tendon of the M. flexor digitorum longus (*MFDL*). It attaches to the cartilage between the second and third phalanx, and to a small line on the proximal surface of the third phalanx (Fig. 5D).

M. gastrocnemius pars lateralis: The M. gastrocnemius pars lateralis (*MGL*, Figs. 2A, 3A, B, 6A) originates muscularly from the caudolateral surface of the external condyle of the femur. Some fibres arise from the lateral surface of the knee joint by a short aponeurosis that is connected with the patellar tendon. The muscle fibres insert on a superficial aponeurosis that merges into the Achilles tendon. This tendon passes the Cartilago tibialis superficially and attaches to most of the caudal surface of the tarsometatarsus, including the hypotarsus.

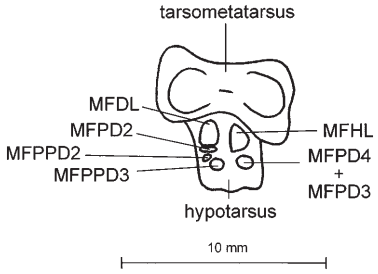

Fig. 4 *Pica pica*, dorsal view of the tarsometatarsus and the hypotarsus. For explanation of abbreviations, see Table 6

b) Medial layer. M. flexor perforans et perforatus digiti 2: The M. flexor perforans et perforatus digiti 2 (*MFPPD2*, Figs. 2B, 4, 5C, 6A) originates tendinously from the caudolateral surface of the external condyle of the femur and is connected with the muscle belly of the Mm. flexor perforatus digiti 2 (*MFPD2*) and flexor perforans et perforatus digiti 3 (*MFPPD3*). Its insertion tendon passes medially through the Cartilago tibialis, beneath the Achilles tendon and medial to the tendon of the M. flexor perforans et perforatus digiti 3. It crosses the hypotarsus between the tendons of the Mm. flexor perforatus digiti 2 (*MFPD2*) (cranial) and flexor perforans et perforatus digiti 3 (caudal, Fig. 4). The tendon continues downwards along the caudal surface of the tarsometatarsus to the plantar surface of the second digit. At the first phalanx, the tendon is perforated by a branch of the tendon of the M. flexor digitorum longus (*MFDL*), and perforates that of the M. flexor perforatus digiti 2. The tendon inserts on the cartilage between the first and second phalanx, and on the proximal end of the second phalanx of digit 2 (Fig. 5C).

M. flexor perforatus digiti 2: The slender M. flexor perforatus digiti 2 (*MFPD2*, Figs. 2A, B, 4, 5B, 6A) originates on the caudoventral surface of the external femoral condyle by a tendon. This tendon is shared with the M. flexor hallucis longus (*MFHL*), the M. flexor perforans et perforatus digiti 3 (*MFPPD3*) and the more superficially situated M. flexor perforans et perforatus digiti 2 (*MFPPD2*). The belly of the M. flexor perforatus digiti 2 is connected to that of the M. flexor hallucis longus. The M. flexor perforatus digiti 2 extends along to the lateral surface of the tarsometatarsus and gives rise to a slender tendon that runs [beneath the tendons of the Mm. flexor perforatus digiti 3 (*MFPD3*) and flexor perforatus digiti 4 (*MFPD4*)] towards the middle of the Cartilago tibialis. From here, it proceeds through a channel in the hypotarsus (Fig. 4). When the tendon reaches the plantar surface of digit 2, it becomes perforated by the tendon of the M. perforans et perforatus digiti 2 and a

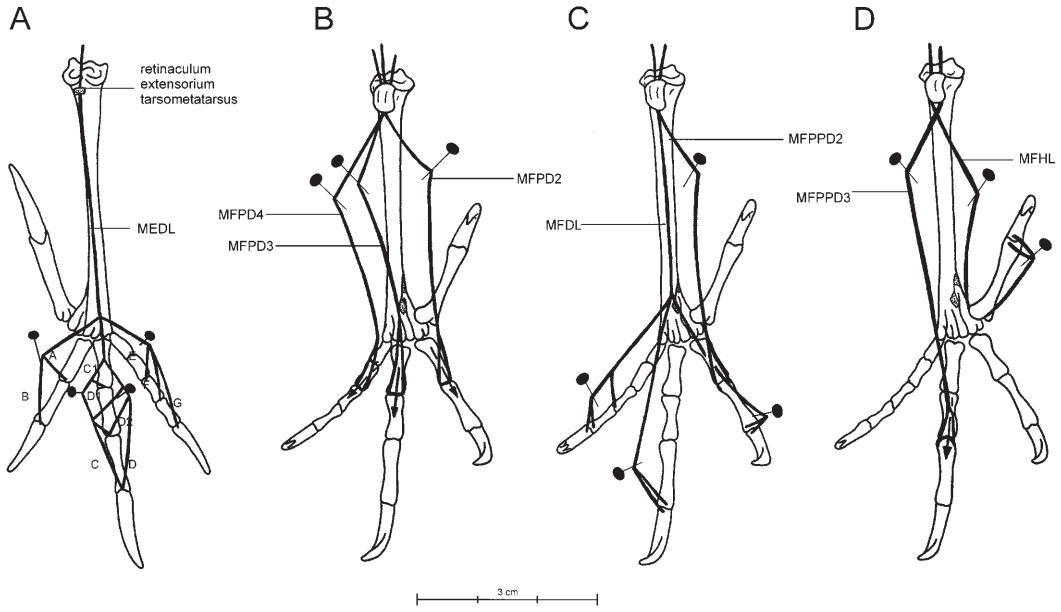

Fig. 5A–D *Pica pica*, schematic drawings of the insertions of the toe flexors and extensors. **A** Dorsal view. **B–D** Ventral views. For explanation of abbreviations, see Table 6

tendon branch of the M. flexor digitorum longus (*MFDL*). The insertion is on the ventral surface of the distal half of the first phalanx (Fig. 5B).

M. flexor perforatus digiti 4: The slender M. flexor perforatus digiti 4 (*MFPD4*, Figs. 2B, C, 3C, 4, 5B) lies on the caudal surface of the lower leg and is bordered laterally by the belly of the M. flexor hallucis longus (*MFHL*) and medially by the M. flexor perforatus digiti 3 (*MFPD3*). The aponeurosis that covers the ventral surface of the muscle is the place of origin of some fibres of the latter muscle. The muscle is covered by the M. gastrocnemius pars intermedia. The muscle originates from the intercondylar region of the femur by a tendon. Just before the ankle joint, the muscle gives rise to a tendon that passes through the Cartilago tibialis at the caudolateral surface where it is partly surrounded by the flattened tendon of the M. flexor perforatus digiti 3 (*MFPD3*). It passes through the ossified channel of the hypotarsus lateral to the tendon of the M. flexor perforans et perforatus digiti 3 (*MFPPD3*) and caudal to that of the M. flexor hallucis longus (*MFHL*, Fig. 4). Below the hypotarsus, the tendon is no longer surrounded by that of the M. flexor perforatus digiti 3. At the base of the plantar surface of the first phalanx of digit 4 it bifurcates, forming a short lateral side branch that inserts on the ventrolateral surface of the distal end of the first phalanx. At the base of the second phalanx, the main branch is perforated by a branch of the tendon of the M. flexor digitorum longus (*MFDL*). The main branch has a broad insertsion on the distal end of the second phalanx and on the cartilage between the second and third phalanges (Fig. 5B).

M. tibialis cranialis: The M. tibialis cranialis (MTC, Figs. 2B, 3A, B, 6C) is situated at the cranial surface of the tibiotarsus. A tibial (MTCT, Fig. 6A) and a femoral head (MTCF) can be distinguished. The former head forms a thin sheet, and arises muscularly from the surface between and on the two crests of the tibiotarsus. The femoral head is covered by the tibial part and arises aponeurotically from the distalmost point of the cranial edge of the external femoral condyle. The femoral and tibial heads fuse halfway along the tibiotarsus to merge into an external tendon that continues along the cranial surface of the tibiotarsus towards the ankle joint. Just above this joint, the tendon of M. tibialis cranialis (together with the tendon of M. extensor digitorum longus, MEDL) passes through the Retinaculum extensorium tibiotarsi (a connective tissue loop at the base of the tibiotarsus, Fig. 1) to cross the ankle joint cranially. It inserts on the cranial surface of the proximal end of the tarsometatarsus.

c) Deep layer M. extensor digitorum longus: The fibres of the M. extensor digitorum longus (*MEDL*, Figs. 2C, 3B, 5A, 6A) originate from the area between the lateral and cranial cnemial crests and from the cranial surface of the proximal part of the tibiotarsus. The internal aponeurosis of the pinnated muscle merges into the external tendon. This tendon extends ventrally and passes, together with the tendon of the M. tibialis cranialis (*MTC*), through the Retinaculum extensorium tibiotarsi. Immediately below this ligament, the tendon passes through an ossified bridge of the tibiotarsus. Just beyond the ankle joint, the tendon continues through the Retinaculum extensorium tarsometatarsus (a small ligamentous loop, Fig. 5A) to extend further ventrally along the cranial surface of the tarsometatarsus. Just above the metatarsophalangeal joint, the tendon trifurcates to the dorsal surface of the three front digits. The insertion of each strand is very complex (Fig. 5A). The branch to digit 2 bifurcates near the base of the first phalanx. The shorter, lateral branch A inserts on the cartilage between the first and the second phalanx. The longest, medial branch B runs

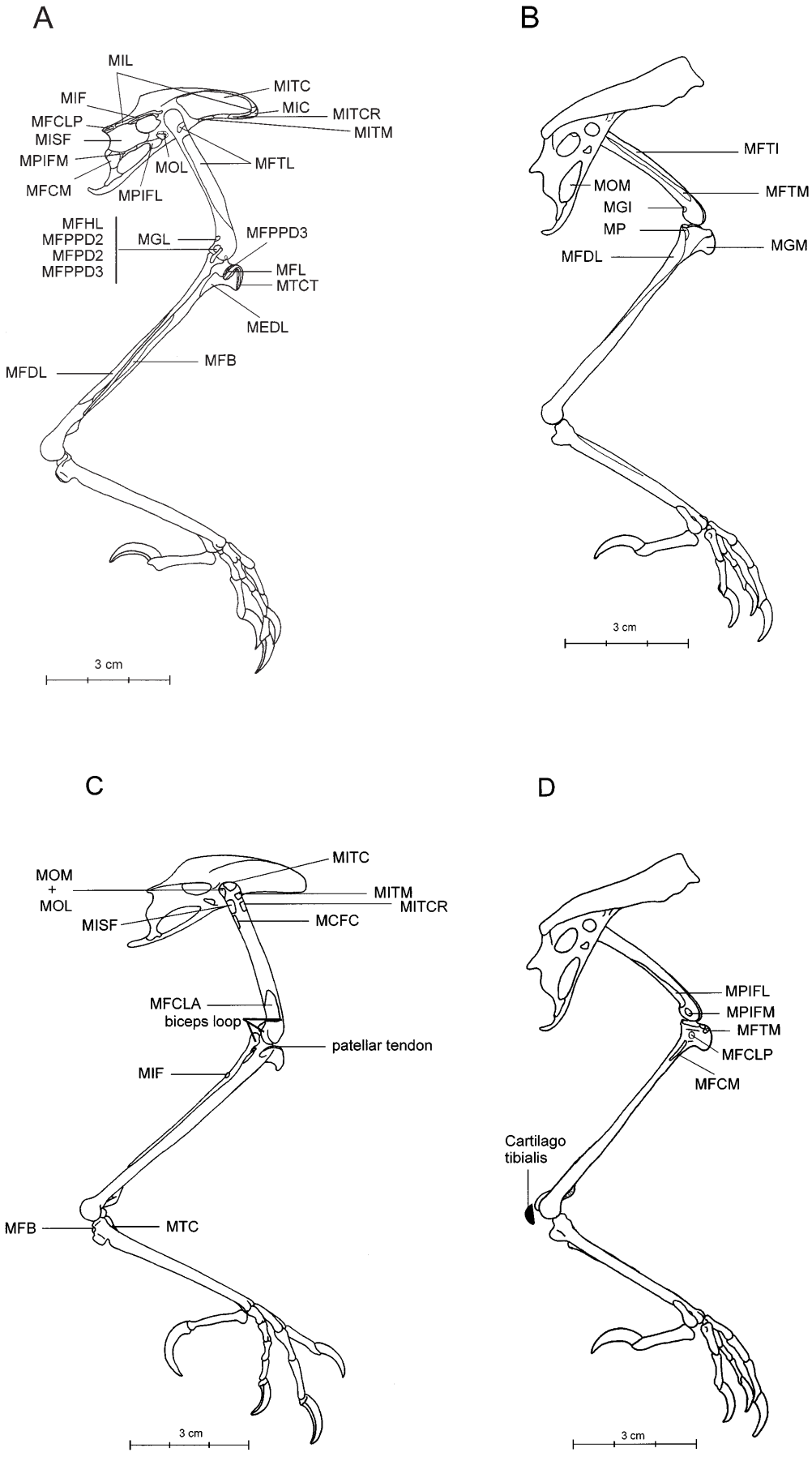

Fig. 6A–D *Pica pica*, origins (**A**, **B**) and insertions (**C**, **D**) of the muscles. **A**, **C** Lateral views. **B**, **D** Medial views. For explanation of abbreviations, see Table 6

distally along the dorsal surface of the digit to insert on the proximal end of the claw. The branch to digit 3 is the widest of the three. At the first phalanx this branch bifurcates to form a medial (C) and lateral (D) branch. Branch C further divides halfway along the first phalanx sending a very short lateral branch (C_1, with a sesamoid) to the proximal end of the second phalanx. The main branch continues distally to fuse with branch D just in front of their common attachment to the proximal border of the claw. Near the base of the second phalanx, the lateral branch D gives rise to a small strand D_1 that fuses over a very short distance with branch C, but readily separates from it again to insert together with D_2 on the base of the third phalanx. The latter is the second split-off of branch D. The branch to digiti 4 trifurcates near the distal end of the first phalanx. The shortest branch (F) lies between the lateral (E) and the medial (G) one. The three branches insert on the proximal end of the third, fourth and ungual phalanx, respectively.

M. fibularis brevis: The M. fibularis brevis (*MFB*, Figs. 2B, C, 6A, C) originates from almost the entire cranial and lateral surface of the fibula and from the adjacent lateral surface of the tibiotarsus. The slender muscle belly runs further downwards along the cranial surface of the tibiotarsus and merges into a tendon. Proximal to the distal end of the tibiotarsus, this tendon passes through Retinaculum m. fibularis (Fig. 1) and continues ventrally to insert on the proximolateral surface of the tarsometatarsus, close to the hypotarsus.

M. flexor digitorum longus: The M. flexor digitorum longus (*MFDL*, Figs. 2C, 3B, C, 4, 5C, 6A, B) forms, together with the M. flexor hallucis longus (MFHL), the so-called 'deep' flexors; their tendons are the 'deep plantar' tendons. Three heads of origin can be distinguished. The fibres from the lateral head originate muscularly and tendinously from the caudal surface of the proximal end of the fibula and the adjacent surface of the tibiotarsus. The fibres from the femoral head originate from the caudal surface of the external femoral condyle. The medial head arises muscularly from the caudomedial surface of the upper two-thirds of the tibiotarsus. Just above the ankle joint, the fused heads merge into a tendon that passes medially through the Cartilago tibialis. It runs through a medial channel at the base of the hypotarsus (Fig. 4). The tendon continues along the caudal surface of the tarsometatarsus. As in other Passeriformes, there is no vinculum between the tendons of the two deep flexors. Just above the metatarsophalangeal joint, the tendon trifurcates, sending one branch to the plantar surface of each of the front digits (Fig. 5C). At the base of the first phalanx of each digit, the branch perforates the other tendons present: on digit 2, the Mm. flexor perforatus digiti 2 (*MFPD2*) and flexor perforans et perforatus digiti 2 (*MFPPD2*), on digit 3, the Mm. flexor perforatus digiti 3 (*MFPD3*) and flexor perforans et perforatus digiti 3 (*MFPPD3*) and on digit 4, the M. flexor perforatus digiti 4 (*MFPD4*). All branches insert on the proximal end of the claw at each digit and send a vinculum to insert on the distal end of the penultimate phalanx. The branch to digit 4 also sends a vinculum to insert on the proximal end of the penultimate phalanx.

M. flexor hallucis longus: The M. flexor hallucis longus (*MFHL*, Figs. 2C, 3C, 4, 5D, 6A) consists of three short heads. Two of them originate by the same tendon that is attached to the external femoral condyle. A thin connective tissue sheet connects it with the proximal part of the fibula. The tendon, however, is perforated by the insertion tendon of the M. iliofibularis (*MIF*). From thereon two heads are distinguished. The third, medial head originates tendinously from the intercondylar region of the femur, distal to the origin of the M. flexor perforatus digiti 3 (*MFPD3*). The heads readily fuse and merge into a tendon that passes through the Cartilago tibialis. It runs laterally through the base of the hypotarsus (Fig. 4). The tendon continues along the caudal surface of the tarsometatarsus and passes between metatarsals 1 and 2 towards the plantar surface of the hallux to insert on the distal end of the first phalanx, via a vinculum, and on the proximal edge of the claw (Fig. 5D).

d) Medially situated muscles M. flexor perforatus digiti 3: The M. flexor perforatus digiti 3 (*MFPD3*, Figs. 3C, 4, 5B) lies on the caudomedial surface of the tibiotarsus, between the Mm. flexor perforatus digiti 4 (*MFPD4*; caudal) and flexor digitorum longus (*MFDL*; cranial). The fibres originate tendinously from the intercondylar region of the femur, lateral and distal to the origin of the M. gastrocnemius pars intermedia (*MGI*). The insertion tendon of the M. flexor perforatus digiti 3 runs downwards and passes along the lateral surface of the Cartilago tibialis, between the Achilles tendon (more superficial) and the tendon of the M. flexor perforatus digiti 2 (*MFPD2*; deeper). At the level of the cartilage the tendon is flattened and partly encloses the tendon of the M. flexor perforatus digiti 4 (*MFPD4*). These two tendons pass together through a channel of the hypotarsus (Fig. 4), whereafter they separate again. At the level of the first phalanx, the tendon of the M. flexor perforatus digiti 3 is perforated by the tendon of the M. flexor perforans et perforatus digiti 3 (*MFPPD3*) and a tendon branch of the M. flexor digitorum longus. The insertion is situated on the plantar surface of the distal part of the first phalanx and on the cartilage between the first and second phalanx (Fig. 5B).

M. gastrocnemius pars intermedia: The origin of the M. gastrocnemius pars intermedia (*MGI*, Figs. 3A, B, 6B) is separated from that of the pars medialis (*MGM*) by the wide, flat insertion tendon of the M. flexor cruris medialis (*MFCM*). The M. gastrocnemius pars intermedia originates muscularly and tendinously from the caudal surface of the internal condyle of the femur. The muscle fibres run to the aponeurotic sheet that merges into the Achilles tendon (see description of the M. gastrocnemius pars lateralis).

M. gastrocnemius pars medialis: The M. gastrocnemius pars medialis (*MGM*, Figs. 3A, 6B) covers the M. gastrocnemius pars intermedia (*MGI*) medially and arises by two heads. The cranial head arises muscularly from

the medial edge of the patellar tendon (the patellar band) and also from the medial surface of the cranial cnemial crest of the tibiotarsus. The caudal head arises from the proximomedial surface of the tibiotarsus. The heads merge and their fibres insert on the aponeurotic sheet forming the Achilles tendon (see description of the M. gastrocnemius pars lateralis).

M. plantaris: The M. plantaris (*MP*, Figs. 3B, 6B) is situated at the medial surface of the tibiotarsus, cranial to the M. gastrocnemius pars intermedia (*MGI*). The origin is covered by the insertion tendon of the M. flexor cruris medialis. The muscle arises muscularly from the caudomedial surface of the proximal end of the tibiotarsus, caudal to the femorotibiotarsal ligament. The muscle fibres merge into a long, slender tendon that continues ventrally towards the Cartilago tibialis to insert on its proximomedial edge.

M. popliteus: The M. popliteus is not present in *Pica pica*. Instead there is a short, strong ligament between the proximal parts of the tibiotarsus and the fibula.

3. Muscles associated with the foot (tarsometatarsus and phalanges, Fig. 1)

M. extensor hallucis longus: The extremely slender M. extensor hallucis longus (*MEHL*) lies on the cranial surface of the tarsometatarsus. It arises muscularly from the cranioproximal part of the tarsometatarsus. At the origin, the muscle is partly covered by the tendon of the M. extensor digitorum longus. Halfway along the tarsometatarsus, the muscle merges into a fine tendon that continues along the caudal surface of metatarsal 1 and the dorsal surface of the hallux to insert on the proximal edge of the claw.

4. Special structures

a) Biceps loop (Fig. 6C). The biceps loop is a strong ligament that surrounds the insertion tendon of the M. iliofibularis (*MIF*) at the caudolateral side knee joint. It has three limbs: one that attaches to the lateral surface of the distal end of the femur just above the external condyle, a second that attaches to the dorsocaudal surface of the external condyle and a third that forms a connection between the second limb and the origin tendon of, among others, the M. flexor perforatus digiti 2 at the level of the proximolateral head of the fibula.

b) Retinaculum extensorium tibiotarsi (Fig. 1). The insertion tendons of the Mm. extensor digitorum longus and tibialis cranialis pass through this oblique loop of ligament. It is situated at the craniocraniomedial surface of the distal end of the tibiotarsus, just above the Pons supratendineus.

c) Bridges of the M. extensor digitorum longus. After passing through the Retinaculum extensorium tibiotarsi, the insertion tendon of the M. extensor digitorum longus passes through the Pons supratendineus, an ossified bridge. Distal to the ankle joint, the tendon passes through the Retinaculum extensorium tarsometatarsi (Fig. 5A), a ligamentous loop situated at the craniomedial surface of the tarsometatarsus. In specimen 3, this loop showed signs of ossification.

d) Ligament of the M. fibularis brevis. The insertion tendon of the M. fibularis brevis passes through the Retinac-

Table 2 Length of leg segments for three specimens of *Pica pica*

Length (cm)	Specimen 5		Specimen 6		Specimen 7	
	Right	Left	Right	Left	Right	Left
Body + head	17.8		15.8		19.1	
Tail	253		22.2		22.6	
Upper leg	4.25	4.28	3.99	3.98	3.92	3.95
Lower leg	6.95	6.93	6.58	6.60	6.71	6.72
Tarsometatarsus	5.00	4.99	4.58	4.58	4.75	4.74
Hallux	2.89	2.83	2.58	2.51	2.64	2.66
Digit 2	2.65	2.62	2.38	2.38	2.55	2.55
Digit 3	2.76	2.65	2.70	2.69	2.51	2.50

Table 3 Total mass and mass of leg segments for three specimens of *Pica pica*

Mass (g)	Specimen 5		Specimen 6		Specimen 7	
	Right	Left	Right	Left	Right	Left
Head + neck	36.19		32.10		34.35	
Trunk + wings	141.06		103.49		127.42	
Tail	1.92		1.80		1.76	
Upperleg	8.11	8.62	6.22	6.11	7.39	7.49
Lowerleg	9.74	9.24	7.06	7.02	8.15	8.22
Tarsometatarsus	1.16	1.16	0.91	0.91	1.02	1.05
Digits	1.12	1.11	0.91	0.91	1.06	1.04
Total specimen	219.43		167.44		198.95	

Table 4 Position of centre of mass (*COM*) of the different body segments as a percentage of the total segment length

Segment	COM (%)	Measured from
Head – neck	59.01	Neck-trunk joint
Trunk – wings	26.53	Neck-trunk joint
Tail	38.30	Trunk-tail joint
Upper leg	47.37	Hip joint
Lower leg	36.51	Knee joint
Tarsometatarsus	47.40	Ankle joint

Table 5 Moments of inertia (*MOI*) of the different body segments for specimen 7

Segment	MOI (kg m^2)	With respect to
Head – neck	4.11E-04	Neck-trunk joint
Trunk – wings	3.08E-04	Hip joint
Tail	5.81E-05	Trunk-tail joint
Upper leg	3.19E-08	Hip joint
Lower leg	6.17E-08	Knee joint
Tarsometatarsus + phalanges	2.94E-08	Ankle joint

Table 6 Morphometrical data of specimen 3. *Abbreviations: A* ankle; *Ca* caudal; *Cr* cranial; *D* distal; *H* hip; *I* interdigital joint; *K* knee; *L* lateral; *LET* length of external tendon; *LIT* length of internal tendon; *M* medial; *Mean FL* mean fiber length; *PA* pinnation angle; *PCS* physiological cross section; *Oss* ossification of tendons. Abbreviations of muscles: *MCFC* musculus caudofemoralis pars caudalis; *MEDL* musculus extensor digitorum longus; *MFB* musculus fibularis brevis; *MFCLA* musculus flexor cruris lateralis pars accessoria; *MFCLP* musculus flexor cruris lateralis pars pelvica; *MFCM* musculus flexor cruris medialis; *MFDL* musculus flexor digitorum longus; *MFHL* musculus flexor hallucis longus; *MFL* musculus fibularis longus; *MFPD2* musculus flexor perforatus d2; *MFPD3* musculus flexor perforatus d3; *MFPD4* musculus flexor perforatus d4; *MFPPD2* musculus flexor perforans et perforatus d2; *MFPPD3* musculus flexor perforans et perforatus d3; *MFTL(I)* musculus femorotibialis lateralis (et intermedius); *MFTI* musculus femorotibialis intermedius; *MFTM* musculus femorotibialis medialis; *MGI* musculus gastrocnemius pars intermedia; *MGL* musculus gastroc-nemius pars lateralis; *MGM* musculus gastrocnemius pars medialis; *MIC* musculus iliotibialis cranialis; *MIF* musculus iliofibularis; *MII* musculus iliofemoralis internus; *MIL* musculus iliotibialis lateralis; *MILmed* musculus iliotibialis lateralis medius; *MILpre* musculus iliotibialis lateralis pars preacetabularis; *MILpost* musculus iliotibialis lateralis pars postacetabularis; *MISF* musculus ischiofemoralis; *MITC* musculus iliotrochantericus caudalis¸*MITCR* musculus iliotrochantericus cranialis; *MITM* musculus iliotrochantericus medius; *MOL* musculus obturatorius lateralis; *MOM* musculus obturatorius medialis; *MP* musculus plantaris; *MPIFL* musculus puboischiofemoralis pars lateralis; *MPIFM* musculus puboischiofemoralis pars medialis; *MTC* musculus tibialis cranialis; *MTCT* musculus tibialis cranialis caput tibiale

Muscle	Mass (g)	Mean FL (mm)	PCS (10^{-6} m^2)	PA (°)	LIT (mm)	LET (mm)	Oss (%)	Position code
MCFC	0.15	23.15	6.17					H_{CaD}
MEDL	0.11	8.97	1.23	17	32.45	104.65		A_{Cr}/I_{Cr}
MFB	0.07	4.55	14.65	14	31.65	13.15		A_{CrL}
MFCLA	0.08	7.62	10.00					H_{Dca}
MFCLP	0.37	25.44	13.85					H_{CaD}/K_{CaM}
MFCM	0.19	18.96	9.54					H_{CaD}/K_{Ca}
MFDL	0.34	8.06	40.18	19	40.20	87.00	31.55	A_{Ca}/I_{Ca}
MFHL	0.42	11.85	33.76	17	28.20	84.15	29.04	$K_{Ca}/A_{Ca}/I_{Ca}$
MFL	0.30	8.29	34.47	21	28.20	27.75		A_{Lca}
MFPD2	0.07	4.66	14.31	9	12.08	80.85	39.13	$(K_{Ca})/A_{Ca}/I_{Ca}$
MFPD3	0.08	5.26	14.49	18	23.15	84.05	36.30	A_{Ca}/I_{Ca}
MFPD4	0.11	5.42	19.33	7	34.00	74.80	40.45	$(K_{Ca})/A_{Ca}/I_{Ca}$
MFPPD2	0.06	6.05	9.45	10		99.85	29.35	$(K_{CaL})/A_{Ca}/I_{Ca}$
MFPPD3	0.22	5.85	35.82	21	33.15	83.25	35.57	$(K_{CaL})/A_{Ca}/I_{Ca}$
MFTL	0.49	10.95	42.62	47	19.79			K_{Cr}
MFTI	0.25	9.69	24.57	30				K_{Cr}
MFTM	0.12	5.82	19.64	19	19.79			K_{CrM}
MGI	0.18	6.90	24.85			49.10		K_{Ca}/A_{Ca}
MGL	0.53	6.91	73.05	23		49.10		K_{CaL}/A_{Ca}
MGM	0.58	11.97	46.15	15		49.10		$(K_M)/A_{Ca}$
MIC	0.31	33.86	8.72					H_{Cr}/K_{Cr}
MIF	0.36	18.72	18.32	17	15.40			H_{Ca}/K_{Ca}
MII	0.01	5.58	1.71					H_{DCr}
MILmed	0.05	9.73	4.89					H_L/K_{LCr}
MILpre	0.11	24.10	4.35	27				H_{LCr}/K_{LCr}
MILpost	0.30	13.78	20.73	33				H_{Lca}/K_{LCr}
MISF	0.14	4.28	31.15					H_{CaL}
MITC	0.29	5.81	47.54		8.95			H_{CrL}
MITCR	0.05	8.05	5.92					H_{CrL}
MITM	0.01	4.16	2.29					H_{CrL}
MOL	0.02	4.26	4.47					H_{Ca}
MOM	0.09	4.97	17.25	19.60	9.40	5.45		H_{Ca}
MP	0.02	6.00	3.17	13.50	8.60			A_{CaP}
MPIFL	0.27	16.56	15.53					H_{CaD}
MPIFM	0.20	10.62	17.94					H_{CaD}
MTCT	0.38	17.53	20.65	13.60	33.25	19.45		A_{Cr}
MTCF	0.18	11.13	15.40	11.90	33.45	19.45		A_{Cr}/K_{Cr}

ulum m. fibularis (Fig. 1), a small ligament situated on the craniolateral surface of the tibiotarsus, lateral to the attachment of the Retinaculum extensorium tibiotarsi.

II. Morphometry

1. Segmental data

Length and mass of the different body segments of three specimens (5–7; see Table 1) are represented in Tables 2 and 3. Table 4 gives the position of the centre of mass as a percentage of the segmental length. Moments of inertia of the segments (with respect to the proximal joint) of specimen 7 (Table 1) are listed in Table 5.

2. Muscle data

Muscular morphometrics are summarised in Table 6. They are obtained from specimen 3 (Table 1). Moment arms are dealt with in the discussion.

D. Discussion

The purpose of this paper is to provide a data set useful for further kinesiological and comparative research on terrestrial locomotion in birds. Data on body dimensions, mass distributions, moments of inertia and centres of mass are indispensable when stride kinematics and dynamographics must be combined to gain insight into the mechanics and energetics of locomotion. Furthermore, profound knowledge of the morphology and morphometrics of the muscle–tendon systems (physiological cross-sections, angles of pinnation, presence and dimensions of internal tendon sheets, location of attachment sites, moment arms, etc.) is needed if one wants to speculate on muscle function in locomotion based on the kinematic patterns and joint dynamics (e.g. Alexander 1974; Alexander and Vernon 1975; Winter 1990a,b; Huijing 1992a,b; Van Leeuwen 1992; Aerts 1998).

I. Morphology

In general, the present description of the leg morphology of *Pica pica* conforms with earlier treatises of hindlimb musculature in corvid birds (Shufeldt 1890; Hudson 1937). This is in agreement with the study of Borecky (1977) who described the limb muscles of 17 corvid species (including *Pica nutalli*) and found that the morphology is very conserved within this family (except for *Pseudopodoces humilis*, based on which it was speculated that this species probably does not belong to the Corvidae).

Only some small differences between *Pica pica* and the corvids (except *Pseudopodoces humilis*) described by Borecky (1977) are noticed. In *Pica pica*, the M. obturatorius lateralis is formed by a single muscle belly. Its division into a dorsal and ventral part by the insertion tendon of the M. obturatorius medialis, as was described by Borecky (1977), is not found in the present dissections. The magpie's M. extensor digitorum longus has one extra insertion on digit 4. The M. popliteus, apparently absent in other Corvidae according to Borecky (1977), is represented in *Pica pica* by a short ligament (see Results). The Mm. flexor hallucis longus and lumbricales are not found in any of the four dissected specimens of *Pica pica*.

Although the standardised nomenclature of the *Nomina Anatomica Avium* (Baumel et al. 1993) is used in the present description, many (functional) morphologists might still be more familiar with terminologies predating this list (e.g. Shufeldt 1890; Hudson 1937; Berger 1960; George and Berger 1966) especially because, for some of the larger leg muscles, the earlier terminology conforms to that of the mammalian nomenclature. As many studies on animal locomotion deal with mammals and treat muscular systems from a functional, rather than from a comparative point of view, Appendix I lists the muscles found in the magpie's leg together with their common synonyms.

II. Muscle function

Although many muscles certainly fulfil an essential stabilising role or cause non-planar leg movements during voluntary complex locomotory behaviour, there is no doubt that most attention must be paid to the sagittal flexion–extension movements of the leg segments, if the propulsion dynamics of straight forward locomotion at constant speeds constitutes the major point of interest (see Introduction). However, muscle function derived from anatomy alone might be prone to misinterpretation of the actual in vivo function as other factors, such as instantaneous leg geometry, co-contractions of other muscles, dynamic constraints (length–tension relation, force–velocity relation, inertial effects), muscle architecture, tendon compliance, timing and level of activation, etc., can have an important impact on the final effect of a muscle contraction. Nevertheless, gross anatomical considerations allow a first functional classification which is useful when further experimental studies have to be undertaken to unravel the precise roles of muscle–tendon systems in the locomotor behaviour. The actions (i.e. flexion and extension) proposed in Appendix II are based on the present dissections and are compared with the interpretations by Hudson (1937), Cracraft (1971), Clark and Alexander (1975) and Raikow (1985). A general agreement in function was found. Muscles crossing more than one joint may show up several times in this list.

Among the variables required for further function analysis, moment arms of muscles are of major importance: a slender muscle with a large moment arm can be a more effective torque generator than a massive one inserting close to the joint. However, moment arms change with the instantaneous configuration of the limb segments throughout the locomotor cycle and with the shifts of the instantaneous centre of rotation of the joints. In principle, measurements should be used that are based on the principle that work done by tendon displacement must be equal to the mechanical work at the rotating joint (e.g. Van Leeuwen 1992). However, the complexity and size of the muscle–tendon system and the rigor of the used specimens made such a procedure not feasible for the present study.

Assigning one single value for a moment arm at a specific joint is rather trivial, except for muscles of which the tendons can be considered as acting along a pulley in the joint (i.e. the moment arm remains constant; e.g. the knee extensors, ankle flexors and ankle extensors). In such cases, a fixed moment arm is estimated from measurement of the skeletal preparations (see further). For other muscles, simple geometric modelling may suffice to obtain relevant estimates for moment arms as a function of the angles of the joint. By expressing the coordinates of the attachment sites of muscles and tendons as a function of the angles of hip and knee, the lines of action of the muscles are defined. Considering this to be the tangent of a circle centred in a crossed joint, the moment arm regarding this joint is given by the

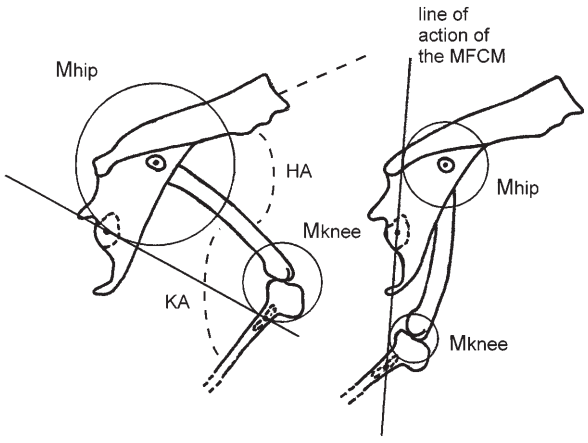

Fig. 7 Example of the boundary conditions used to estimate moment arms of muscles as a function of the hip and knee angle (*HA, KA*). The line of action of the MFCM connects the centres of the attachment sites on the pelvic girdle and the lower leg, respectively. The radii of the circles centred on hip (M_{hip}) and knee (M_{knee}), and touching the line of action, represent the moment arms about hip and knee, respectively. It is obvious that these moment arms will change with changes in HA and/or KA. *Dotted line* represents segmental axis determined by hip and dorsal side of the neck

Table 7 Parameter values (*a–d*, α, β) to calculate moment arms

Muscle	a	b	c	d	α	β
MFCM	0.00	0.00	0.17	0.41	3.17	3.71
MIF	–0.13	0.79	0.00	0.14	0.00	3.13
MFCLP	0.00	0.00	0.11	0.39	3.01	3.35
MPIFL	0.03	0.48	0.00	0.17	0.00	3.86
MPIFM	0.31	0.72	0.00	0.29	0.00	3.78
MIT	0.10	0.85	0.00	0.47	0.00	0.23

circle's radius. With respect to the hip and knee, moment arms are given by the mathematical expression of this boundary condition (see Fig. 7):

$$\text{Moment arm}_{hip} = (t^2/(1+m^2))^{0.5}$$

$$\text{Moment arm}_{knee} = ((0.85\ m+t)^2/(1+m^2))^{0.5}$$

(where appropriate; see further),

where $m=(a+c\ \sin(KA+\alpha)–d\ \sin(HA+\beta))/(b+c\ \cos(KA+\alpha)–d\ \cos(HA+\beta)+0.85)$ and $t=–d\ \cos\ (HA+\beta)\ m+d\ \sin(HA+\beta)$. In these formulae, the variables KA and HA are the knee angle and hip angle, respectively. The values for the parameters a, b, c, d, α and β are muscle dependent and are given for six muscles important in flexion and/or extension of hip and knee in Table 7 (see Fig. 7). To frame these constants, linear dimensions were normalised to tarsometatarsal length (standard measure in birds; Svensson 1992). Thus, the obtained moment arms are also expressed as a fraction of the tarsometatarsal length. The knee angle is defined by the long axis of the femur and tibiotarsus (at the back side of the leg, see Fig. 7), and the hip angle by the long axis of the femur and the axis from the hip to the dorsal side of the neck (this segment definition is also used for the kinematic analysis, see Fig. 7). For the purpose of understanding the general function of muscle groups in locomotion, this approach proved to be reliable and useful (see for example Aerts 1998). To analyse the role of a specific muscle in all its details, more precise measurements of the varying moment arm might be required.

1. Leg extension

Extensions of the hip, knee and ankle joints are likely to be involved in the power phase of the locomotor cycles. The massive hamstrings (M. flexor cruris lateralis pars pelvica and M. iliofibularis, M. flexor cruris medialis) and the Mm. puboischiofemoralis are the most important hip extensors both in terms of mass and physiological cross-section. Moment arms of these muscles, with respect to the hip, will change during extension according to the geometry of the system (see Table 6). Knee extension results from contraction of the bundles of the M. femorotibialis and M. iliotibialis and these muscles act on the patellar tendon. A moment arm of about 5 mm can be estimated from the skeletal preparation of a specimen with a tarsometatarsal length of 46 mm. The gastrocnemius (three parts) is the most important ankle extensor. Its medial and lateral parts are by far the largest and most forceful muscle bundles in the leg (as judged by the physiological cross section). This is in accordance with the findings for the quail (*Coturnix coturnix*: Clark and Alexander 1975). As the long tendons of the flexors of the digits are guided along the Cartilago tibialis and through the hypotarsus at the back of the tibiotarsus and tarsometatarsus, these muscles are also assumed to contribute considerably to ankle extension (cf. Clark and Alexander 1975). All these toe flexors together are about as massive and forceful as the three bundles of the M. gastrocnemius. Moreover, since the tendons of the toe flexors act along the 'pulley' formed by the cartilage and the hypotarsus, which are also directly covered by the broad Achilles tendon, the moment arms of the toe flexors and the M. gastrocnemius bundles must be more or less identical. As a result, it can be postulated that the M. gastrocnemius bundles and the toe flexors are equally important in forceful ankle extension for locomotion. For a leg with a tarsometatarsal length of 46 mm, the averaged moment arm of the ankle extensors is estimated to be about 5 mm. Manipulation of the skeletal preparation suggests that the instantaneous centre of rotation shifts backwards during ankle extension, whereby the length of the moment arm decreases.

2. Leg flexion

As judged by its position with respect to the hip and its size, the large M. iliotibialis cranialis can safely be assumed to be the most important hip flexor. As in the pigeon (*Columba livia*: Cracraft 1971), the massive M. iliotrochantericus caudalis cannot be considered as a

femoral protractor because the muscle inserts at the level of the hip joint (see also Raikow 1985). The hamstrings flex the knee. The bundles of the M. gastrocnemius are believed not to participate in any significant way in knee flexion as the biarticular bundles insert almost laterally and very close to the knee joint (see Results), which makes the moment arm for the knee small, and torques negligible. Also, in the quail (Clark and Alexander 1975) and the pigeon (Cracraft 1971), knee flexing moments by the bundles of the M. gastrocnemius are assumed to be unimportant. The moment arms of these hip and knee flexors (except for the M. iliofibularis) will change during flexion according to the particular geometry of the system during the movement cycles (see Table 7; Fig. 7). In case of the M. iliofibularis, the orientation of the insertion tendon is determined by the biceps loop which makes the moment arm at the knee independent of the configuration of the leg segments. It is estimated to be 5 mm for a leg with a tarsometatarsal length of 46 mm. The ankle is flexed by the M. tibialis cranialis. Contraction of the M. extensor digitorum longus also adds to ankle flexion. The tendons of both muscles are constrained by several ligamentous and bony bridges at the level of the joint (among others the Retinacula extensorium tibiotarsi and tarsometatarsus; see Results). Therefore, the moment arms of these extensor muscles will be fairly similar to each other and are estimated on the skeletal preparation to be less than 2.5 mm for a specimen with a tarsometatarsus of 46 mm.

III. Muscle architecture

As far as we know, only Cracraft (1971) and Clark and Alexander (1975) present morphometric data for leg muscles in birds. The former provides measurements of pinnation angles and fibre length (measured on intact preserved muscles, fixed in a standing position), as well as estimates of the number of fibres (as a relative measure of force) and moment arms (for the standing position) of the pigeon. Clark and Alexander (1975) provide measurements of mass and pinnation angles (measured on histological sections), and estimates of cross-sectional area and moment arms (measured on X-rays) for those muscles of the quail (0.095 kg) that seem likely to exert substantial forces during running. Only for the parallel-fibred muscles are cross-sectional areas directly comparable to the physiological cross-section as given in the present paper (see Table 6). For pinnate muscles, the figures by Clark and Alexander (1975) should be divided by the cosine of the pinnation angle in order to obtain cross-sectional area perpendicular to the muscle fibres (i.e. physiological cross-section as used in this paper).

In general, the appearance of muscle pinnation in the leg muscles seems to be similar for the magpie, the quail (Clark and Alexander 1975) and the pigeon (Cracraft 1971). The M. iliofibularis and the M. iliotibialis lateralis form noticeable exceptions. The first is pinnate only in the magpie and the second is parallel fibred in the quail. The pinnation angles vary between the species. This might reflect actual differences, but may also result from the differences in procedure (histological sections versus macroscopic sectioning).

Table 6 lists muscles for which ossifications in the long tendons occur (see also Olmos et al. 1993). Intratendinous ossifications do not seem to affect the tensile strength, but increase the stiffness of tendons considerably (Bennett and Stafford 1988; Olmos et al. 1993). Therefore, it is concluded that tendon ossifications mainly function in avoiding stretching of long tendons during normal behaviour (Bennett and Stafford 1988; Vanden Berge and Storer 1995). Shortening of the muscle belly is thus transmitted to the target joints without any loss of displacement (rotation) due to tendon compliance. This is especially important for short-fibred, pinnate muscles for which the muscle strain is limited (extension of too compliant tendons should compensate for all muscle shortening) and for muscles with tendons running close to the centre of rotation of the joints (tendon compliance should readily hamper joint extension). In the magpie, only the toe flexors show ossifications. These muscles have short fibres, are pinnate and the tendons run just underneath the joints.

One of the consequences of tendon ossification is that the potential for energy saving during locomotion by elastic tendon recoil is largely reduced (Bennett and Stafford 1988). But, since the mechanical properties of non-ossified avian tendons are similar to those of mammalian tendon (Bennett and Stafford 1988), it is inferred that elastic recoil does not play an important role in terrestrial locomotion of small birds anyway (Biewener et al. 1981; Hayes and Alexander 1983; Van Leeuwen 1992). From this point of view, fewer ossifications in heavy, cursorial birds, such as the turkey (*Meleagris gallopavo*) (up to more than 30 kg) should be expected. Surprisingly, in this species, tendon ossification is extensive (cf. Hudson et al. 1959). Even the tendon of the M. gastrocnemius (the forceful ankle extensor) is ossified. This is not the case for *Pica pica*. Here, the Achilles tendon is not ossified and has thus kept its energy-saving potency.

III. Segmental data

For dynamic modelling, the segmental data presented in this paper (mass and position of centre of mass, moment of inertia) are needed, together with detailed information on segmental displacement and ground reaction forces during locomotion. The mechanical energy delivered in locomotion is usually split into external and internal work. The former relates to the costs for the movements of the centre of mass of the total body; the latter to the movements of the body with respect to that total centre of mass. If the masses of body segments are much smaller than the total mass (and, consequently, also the moments of inertia), the internal work components related

to the displacements of these segments will be negligible in the total energy budget. Tables 3 and 5 show that the masses and especially the moments of inertia of all leg segments are small compared to those of the head and trunk. The masses amount to only a small percentage of the total body mass, whereas the moments of inertia are about 10^4 times smaller than those of the trunk and head. Therefore, it can be assumed that, in calculating the mechanical costs of locomotion in *Pica pica*, energy fluctuations coupled to leg movements (i.e. internal work) will be negligible (unless linear and angular accelerations should be unrealistically high). This implies that, for the purpose of comparing different gaits, a reliable estimate of the mechanical costs will be obtainable from the energy fluctuations of the centre of mass alone. Such data can easily be computed when the measurements of ground reaction forces are available. Only for gaits characterised by considerable roll and/or pitch and/or yaw of the body, additional energy components may need to be added. Kinematic analysis must bring a decisive answer to this.

Appendix I (common synonyms)

Baumel et al. (1993)	(1) Hudson (1937); (2) Berger (1960); (3) Shufeldt (1890)
Caudofemoralis pars caudalis	Piriformis (1,2); femorocaudalis (3)
Extensor digitorum longus	Extensor longus digitorum (3)
Femorotibialis intermedius	Cruraeus (3)
Femorotibialis lateralis	Vastus externus (3)
Femorotibialis medialis	Vastus internus (3)
Fibularis brevis (peroneus brevis)	Tibialis posticus (3)
Fibularis longus (peroneus longus)	(1,2,3)
Flexor cruris lateralis pars accessoria	Accessorius semitendinosi (1,2,3)
Flexor cruris lateralis pars pelvica	Semitendinosus (1,2,3)
Flexor cruris medialis	Semimembranosus (1,2,3)
Flexor digitorum longus	Flexor perforans digitorum profundus (3)
Flexor hallucis longus	Flexor longus hallucis (3)
Flexor perforans et perforatus digiti 3	Flexor perforatus medius secundus pedis (3)
Flexor perforans et perforatus digiti 2	Flexor perforatus indicis secondus pedis (3)
Flexor perforatus digiti 2	Flexor perforatus indicis primus pedis (3)
Flexor perforatus digiti 3	Flexor perforatus medius primus pedis (3)
Flexor perforatus digiti 4	Flexor perforatus annularis primus pedis (3)
Gastrocnemius pars intermedia	Gastrocnemius pars media (1,2)
Gastrocnemius pars lateralis	Gastrocnemius pars externa (1,2)
Gastrocnemius pars medialis	Gastrocnemius pars interna (1,2)
Iliofemoralis internus	Iliacus (1,2)
Iliofibularis	Biceps femoris (1,2); biceps flexor cruris (3)
Iliotibialis cranialis	Sartorius (1,2,3)
Iliotibialis lateralis	Iliotibialis (1,2); gluteus primus (3)
Iiliotrochantericus caudalis	Iliotrochantericus posterior (1,2); gluteus medius (3)
Iliotrochantericus cranialis	Iliotrochantericus anterior (1,2); gluteus minimus(3)
Iliotrochantericus medius	(1,2,3)
Ischiofemoralis	Obturator externus (3)
Obturatorius lateralis	Obturator externus (1,2); gemellus (3)
Obturatorius medialis	Obturator internus (1,2,3)
Plantaris	Soleus (3)
Puboischiofemoralis pars medialis	Adductor longus et brevis pars posterior (1,2); adductor magnus (3)
Puboischiofemoralis pars lateralis	Adductor longus et brevis pars anterior (1,2); adductor longus (3)
Tibialis cranialis caput tibiale	Tibialis anterior (1,2); tibialis anticus (3)

Appendix II

	Mass	Fraction	PCS	Fraction
Hip extensors				
Puboischiofemoralis pars medialis	0.203	0.027081109925293	20.2	0.028861265895128
Puboischiofemoralis pars lateralis	0.273	0.036419423692636	18.3	0.026146592370339
Flexor cruris lateralis pars pelvica	0.374	0.049893276414088	16.5	0.023574796399486
Iliofibularis	0.359	0.047892209178228	15.8	0.022574653521932
Obteratorius medialis	0.091	0.012139807897545	13.3	0.019002714673525
Flexor cruris medialis	0.189	0.025213447171825	9.8	0.014002000285755
Flexor cruris lateralis pars accessoria	0.078	0.010405549626467	9.4	0.01343049007001
Caudofemoralis pars caudalis	0.145	0.019343649946638	5.5	0.0078582654664952
Obteratorius lateralis	0.025	0.0033351120597652	4.9	0.0070010001428776

	Mass	Fraction	PCS	Fraction
Knee extensors				
Femorotibialis lateralis	0.489	0.065234791889007	36.1	0.051578796970996
Iliotibialis lateralis	0.463	0.061766275346852	23.6	0.033719102728961
Femorotibialis intermedius	0.247	0.03295090715048	17.7	0.025289327046721
Iliotibialis cranialis	0.305	0.040688367129136	7.3	0.010430061437348
Ankle extensors				
Gastrocnemius pars lateralis	0.531	0.070837780149413	72.0	0.10287183883412
Gastrocnemius pars medialis	0.580	0.077374599786553	50.2	0.071724532076011
Flexor digitorum longus	0.336	0.044823906083244	43.6	0.062294613516217
Fibularis longus (peroneus longus)	0.302	0.040288153681964	41.6	0.059437062437491
Flexor hallucis longus	0.419	0.055896478121665	32.0	0.045720817259609
Flexor perforans et perforatus digiti 3	0.219	0.029215581643543	32.0	0.045720817259609
Gastrocnemius pars intermedia	0.179	0.023879402347919	24.9	0.035576510930133
Flexor perforatus digiti 4	0.106	0.014140875133404	18.2	0.026003714816402
Flexor perforatus digiti 2	0.068	0.0090715048025614	14.5	0.02071724532076
Flexor perforatus digiti 3	0.078	0.010405549626467	12.9	0.01843120445778
Fibularis brevis (peroneus brevis)	0.067	0.0089381003201708	11.1	0.015859408486927
Flexor perforans et perforatus digiti 2	0.058	0.0077374599786553	10.1	0.014430632947564
Plantaris	0.024	0.0032017075773746	4.50	0.0064294899271324
Digital extensors				
Extensor digitorum longus	0.113	0.015074706510139	9.50	0.013573367623946
Hip flexors				
Iliotrochantericus caudalis	0.293	0.039087513340448	40.5	0.057865409344192
Iliotibialis cranialis	0.305	0.040688367129136	7.30	0.010430061437348
Iliotrochantericus cranialis	0.052	0.0069370330843116	4.50	0.0064294899271324
Iliotrochantericus medius	0.006	0.00080042689434365	1.10	0.001571653093299
Iliofemoralis internus	0.006	0.00080042689434365	0.80	0.0011430204314902
Knee flexors				
Flexor cruris lateralis pars pelvica	0.374	0.049893276414088	16.5	0.023574796399486
Iliofibularis	0.359	0.047892209178228	15.8	0.022574653521932
Flexor cruris medialis	0.189	0.025213447171825	9.80	0.014002000285755
Ankle flexors				
Tibialis cranialis	0.376	0.050160085378869	17.6	0.025146449492785
Tibialis cranialis caput femorale	0.178	0.023745997865528	12.5	0.017859694242035
Extensor digitorum longus	0.113	0.015074706510139	9.50	0.013573367623946
Digital flexors				
Gastrocnemius pars lateralis	0.531	0.070837780149413	72.0	0.10287183883412
Gastrocnemius pars medialis	0.580	0.077374599786553	50.2	0.071724532076011
Flexor digitorum longus	0.336	0.044823906083244	43.6	0.062294613516217
Fibularis longus (peroneus longus)	0.302	0.040288153681964	41.6	0.059437062437491
Flexor perforans et perforatus digiti 3	0.219	0.029215581643543	32.0	0.045720817259609
Flexor hallucis longus	0.419	0.055896478121665	32.0	0.045720817259609
Gastrocnemius pars intermedia	0.179	0.023879402347919	24.9	0.035576510930133
Flexor perforatus digiti 4	0.106	0.014140875133404	18.2	0.026003714816402
Flexor perforatus digiti 2	0.068	0.0090715048025614	14.5	0.02071724532076
Flexor perforatus digiti 3	0.078	0.010405549626467	12.9	0.01843120445778
Flexor perforans et perforatus digiti 2	0.058	0.0077374599786553	10.1	0.014430632947564

Acknowledgements The authors wish to thank Dr. A. Herrel (Antwerp University, Belgium) for his comments on the manuscript. We acknowledge G. Verbeylen for her assistance in obtaining dissection material. M. Verstappen is funded by IWT-grant SB 961234. P. Aerts is Research Director of the Fund for Scientific Research – Flanders (Belgium).

References

Aerts P (1998) Vertical jump in *Galago senegalensis*: the quest for a hidden power amplifier. Philos Trans R Soc Lond Biol Sci 353

Alexander RMcN (1974) The mechanics of jumping by a dog, *Canis familiaris*. J Zool Lond 173:549–573

Alexander RMcN (1976) Mechanics of bipedal locomotion. In: Spencer Davies P (ed) Perspectives in animal biology. Pergamon Press, Oxford

Alexander RMcN (1977a) Mechanics and scaling of terrestrial locomotion. In: Pedley TJ (ed) Scale effects in animal locomotion. Part II: Terrestrial locomotion. Academic Press, London

Alexander RMcN (1977b) Terrestrial locomotion. In: Alexander RMcN, Goldspink G (eds) Mechanics and energetics of animal locomotion. Wiley and Sons, New York

Alexander RMcN (1983) Animal mechanics, 2nd edn. Blackwell Scientific, Oxford

Alexander RMcN (1992) Exploring biomechanics. Animals in motion. Scientific American Library, New York

Alexander RMcN, Vernon A (1975) The mechanics of hopping by kangaroos (Macropodidae). J Zool Lond 177:265–303

Alexander RMcN, Maloiy GMO, Njau R, Jayes AS (1979) Mechanics of running of the Ostrich (*Struthio camelus*). J Zool Lond 187:169–178

Alexander RMcN, Jayes AS, Ker RF (1980) Estimates of energy cost for quadrupedal running gaits. J Zool Lond 190:155–192

Baumel JJ, King AS, Lucas AM, Breazile JE, Evans HE, Vanden Berge JC (1993) Handbook of avian anatomy. Nomina Anatomica Avium II. Nuttal Ornithol Club Publ 23, Cambridge Mass

Bennett MB (1992) Empirical studies of walking and running. In: Alexander RMcN (ed) Advances in comparative and environ-

mental physiology, vol 11. Mechanics of animal locomotion. Springer, Berlin Heidelberg New York
Bennett MB, Stafford JA (1988) Tensile properties of calcified and uncalcified avian tendons. J Zool Lond 214:343–351
Berger AJ (1960) The musculature. In: Marshall AJ (ed) Biology and comparative physiology of birds, vol 1. Academic Press, New York
Biewener AA, Alexander RMcN, Heglund NC (1981) Elastic energy storage in the hopping of the Kangaroo Rats (*Dipodomys spectabilis*). J Zool Lond 195:369–383
Blickhan R (1989) The spring-mass model for running and hopping. J Biomech 22:1217–1227
Borecky SR (1977) The appendicular myology and phylogenetic relationships of the avian 'Corvid assemblage'. PhD dissertation, University of Pittsburgh, Pittsburgh
Cavagna GA, Heglund NC, Taylor CR (1977) Mechanical work in terrestrial locomotion: two basic mechanisms for minimizing energy expenditure. Am J Physiol 233:R243–R261
Clark GA Jr (1975) Additional records of passerine terrestrial gaits. Wilson Bulletin 87:384–389
Clark J, Alexander RMcN (1975) Mechanics of running by quail (*Coturnix*). J Zool Lond 176:87–113
Cracraft J (1971) The functional morphology of the hind limb of the domestic pigeon, *Columba livia*. Bull Am Mus Nat Hist 144:175–265
Dagg AI (1977) The walk of the silver gull (*Larus novaehollandiae*) and of other birds. J Zool Lond 182:529–540
Farley CT, Taylor CR (1991) A mechanical trigger for the trot-gallop transition in horses. Science 253:306–308
Farley CT, Glasheen J, McMahon TA (1993) Running springs: speed and animal size. J Exp Biol 185:71–86
George JC, Berger AJ (1966) "Avian myology". Academic Press, New York
Hayes G, Alexander RMcN (1983) The hopping gaits of crows (Corvidae) and other bipeds. J Zool Lond 200:205–213
Hoyt DF, Taylor CR (1981) Gait and the energetics of locomotion in horses. Nature 292:239–240
Hreljac A (1993a) Preferred and energetically optimal gait transition speeds in human locomotion. Med Sci Sports Exerc 25:1158–1162
Hreljac A (1993b) Determinants of the gait transition speed during human locomotion: kinetic factors. Gait Posture 1993:217– 223
Hreljac A (1995a) Determinants of the gait transition speed during human locomotion: kinematic factors. J Biomech 28:669–677
Hreljac A (1995b) Effects of physical characteristics on the gait transition speed during human locomotion. Hum Movement Sci 14:205–216
Hudson GE (1937) Studies on the muscles of the pelvic appendage in birds. Am Midland Nat 18:1–108
Hudson GE, Lanzillotti PJ, Edwards GD (1959) Muscles of the pelvic limb in Galliform birds. Am Midland Nat 61:1–67
Huijng PA (1992a) Mechanical muscle models. In: Komi PV (ed) Strength and power in sport, vol 3. Blackwell Scientific Publications, Oxford
Huijng PA (1992b) Elastic potential of muscle. In: Komi PV (ed) Strength and power in sport, vol 3. Blackwell Scientific Publications, Oxford
Kram R, Domingo A, Ferris DP (1997) Effect of reduced gravity on the preferred walk-run transition speed. J Exp Biol 200:821–826
Kunkel P (1962) Zur Verbreitung des Hüpfens und Laufens unter Sperlingsvögeln (Passeres). Z Tierpsychol 19:417–439
Loeb GE, Gans C (1986) Electromyography for experimentalists. University of Chicago Press, Chicago
McMahom TA (1984) Muscles, reflexes and locomotion. Princeton University Press, Princeton NJ
Minetti AE, Alexander RMcN (1997) A theory of metabolic costs for bipedal gaits. J Theor Biol 186:467–476
Minetti AE, Saibene F (1992) Mechanical work rate minimization and freely chosen stride frequency of human walking: a mathematical model. J Exp Biol 170:19–34
Mochon S, McMahon TA (1980) Ballistic walking. J Biomech 13:49–57
Olmos M, Planell JA, Casinos A (1993) Tensile fracture loads of leg tendons in birds. Ann Sci Nat Zool Paris 13th Ser 14:23–33
Peters JL (1987) Checklist of the birds of the world. Harward University, Harward, USA
Raikow RJ (1985) Locomotor system. In: King AS, McLelland J (eds) Form and function in birds, vol 3. Academic Press, London
Roberts TJ, Marsh RL, Weyland PG, Taylor RC (1997) Muscular force in running turkeys: the economy of minimizing work. Science 275:1113–1115
Rylander MK, Bolen EG (1974) Analysis and comparison of gaits in whistling ducks (*Dendrocygna*). Wilson Bull 86:237–245
Shufeldt RW (1890) The myology of the Raven (*Corvus corax sinatus*). MacMillan, London
Smith RM (1987) Biomechanics of the locomotion of *Galago senegalensis*. PhD Arizona State University, Mich
Svensson L (1992) Identification guide to European Passerines (4th edn). Svensson, Stockholm
Taylor MA (1994) Stone, bone or blubber? Buoyancy control strategies in aquatic tetrapods. In: Maddock L, Bone Q, Rayner JMV (eds) Mechanics and physiology of animal swimming. Cambridge University Press, Cambridge
Vanden Berge JC, Storer RW (1995) Intratendinous ossification in birds: a review. J Morphol 226:47–77
Van Leeuwen JL (1992) Muscle function in locomotion. In: Alexander RMcN (ed) Comparative and environmental physiology, vol 11. Mechanics of animal locomotion. Springer, Berlin Heidelberg New York
Webb GJW, Gans C (1982) Galloping in *Crocodylus johnstoni*, a reflection of terrestrial activity? Rec Aust Mus 34:607–618
Winter DA (1990a) The biomechanics and motor control of human gait: normal, elderly and pathological. University of Waterloo Press, Waterloo
Winter DA (1990b) Biomechanics and motor control of human movement. Wiley and Sons, New York